

Study Committee B2
PS2 Latest Techniques in Asset Management, Capacity
Enhancement, Refurbishment

**Experimental Study of Dynamic Bending Stiffness of Typical Overhead
Conductor with Formed Wires**

Zhao ZHANG*, Shengchun LIU, Yi QI, Jian ZHANG, Zhen LIU, Long LIU
China Electric Power Research Institute
China

**zhangzhao@epri.sgcc.com.cn, liushengchun@epri.sgcc.com.cn, qiyi@epri.sgcc.com.cn,
zhangjian@epri.sgcc.com.cn, liuzhen@epri.sgcc.com.cn, liulong@epri.sgcc.com.cn**

SUMMARY

With the economic development and the growth of social demand for electricity in recent year, the scale of China's power grid is getting larger and larger. Transmission lines of 110 (66) kV and above have been built in the country for about 1.1 million kilometers. The lines not only suffer from icing, galloping, aeolian vibration and other problems in a complex and diverse natural environment, but also face the requirements of improved transmission capacity and conductor sag characteristics. Therefore, a series of new overhead conductors are developed, such as carbon fiber composite core reinforced conductors and formed wire concentric-lay-stranded conductors, which use formed wires.

Overhead conductor is made of a set of metal single wires. In the actual lines, the conductor is almost always subject to aeolian vibration. The long-term vibration can lead to fatigue failure of the conductor and even the line breakage. The dynamic bending stiffness of conductor has an important influence on the deformation and fatigue characteristics of conductor near the clamp when aeolian vibration occurs. It depends on the friction between the adjacent single wires of the conductor. There is nonlinear slip between single wires and layers during conductor vibration, which makes the calculation of bending stiffness very complicated. Under the condition of no slip, the maximum stiffness of the conductor can be calculated. And when the friction between strands is not considered, it can achieve the minimum bending stiffness. However, there are tens or even hundreds of times difference between the maximum bending stiffness and the minimum value of the conductor. For conductors with formed wires, the section of some single wires may be irregular, so the calculation becomes more difficult. Therefore, the bending stiffness evaluation of conductors with formed wires base on experiment is a problem worthy of study.

Some scholars have done a lot of research on the evaluation of the bending stiffness of the traditional round wire concentric-lay-stranded conductor, and have achieved good applications. There are relatively few reports on the evaluation of the dynamic bending stiffness of the conductors with formed wires. In order to further study the evaluation method of dynamic bending stiffness of these conductors, a typical carbon fiber composite core reinforced conductor is selected. The indoor aeolian vibration simulation test system with a span of 140 m is used to measure the amplitude and the strain of the conductor under different conditions. The amplitudes are measured at the first antinode from the fixed end, where a rigid square-faced bushing is used, on the cable test bench. The strain is measured

at the last point of contact of the conductor with the fixed end. The measurement results are substituted into the dynamic bending strain model of the conductor, and the method of the dynamic bending stiffness evaluation of the conductor is obtained. The research is of great significance to improve the reliability of the fatigue test of the conductors with formed wires and to provide valuable data for the numerical simulation of conductor aeolian vibration.

KEYWORDS

Overhead conductor - Formed wire - Dynamic bending stiffness - Experimental study

1. PRINCIPLE OF DYNAMIC BENDING STIFFNESS EVALUATION

1.1 Model of the dynamic bending strain

In case of aeolian vibration of the conductor, the forces and the moments on the conductor micro element are shown in Fig. 1. For the sake of analysis, it is assumed that the conductor is rigid and undamped.

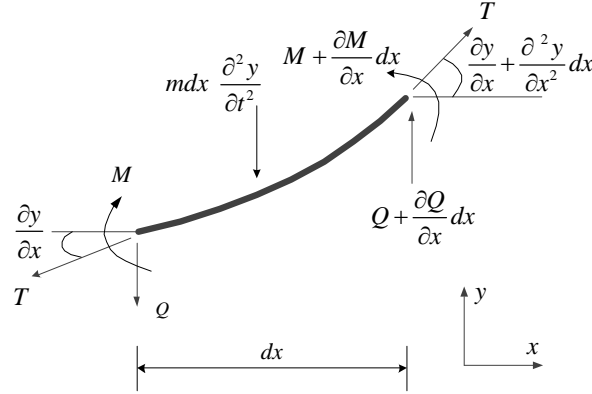


Fig. 1 Force model of conductor under aeolian vibration

According to the force and moment balance conditions of conductor micro element in Fig. 1, the equation can be listed as follows[1] :

$$\begin{cases} m \frac{\partial^2 y}{\partial t^2} - T \frac{\partial^2 y}{\partial x^2} - \frac{\partial Q}{\partial x} = 0 \\ Q + \frac{\partial M}{\partial x} = 0 \end{cases} \quad (1)$$

In equation (1), m is the conductor mass per unit length (kg/m); T is the conductor tension (N). Q is the shear force on conductor element (N), and M is the bending moment on conductor element (N.m),

$$M = EI \frac{\partial^2 y}{\partial x^2} \quad (2)$$

In equation (2), EI is the global dynamic bending stiffness of the conductor (N.m²). Substituting equation (2) into equation (1), the differential equation of free vibration of conductor is obtained, which is shown as follows,

$$EI \frac{\partial^4 y}{\partial x^4} + m \frac{\partial^2 y}{\partial t^2} - T \frac{\partial^2 y}{\partial x^2} = 0 \quad (3)$$

For convenience, it is assumed that both ends of conductor are simply supported, the natural frequency ω_n of the conductor is obtained by solving the differential equation above,

$$\omega_n = \frac{n\pi}{L} \sqrt{\frac{T}{m}} \sqrt{1 + \frac{n^2 \pi^2 EI}{L^2 T}} \quad (4)$$

In equation (4), n is the number of half waves in the span (approximately equal to the corresponding order of the natural frequency), and L is the span length (m). The maximum dynamic bending stress at the outlet of the conductor clamp can be derived, which is shown as follows [2],

$$\sigma_{\max} = \frac{RE_a y_{\max} (r^2 + s^2)}{2[(s/r)^2 + 1]^{1/2}} \quad (5)$$

In equation (5), R is the radius of conductor (m); E_a is the elastic modulus of aluminium (Pa); y_{\max} is the antinode amplitude of the conductor (m); σ_{\max} is the maximum dynamic bending stress of the

conductor at the outlet of the clamp (Pa); r and s are intermediate variables, which is described as follows,

$$\begin{cases} r = [(q^4 + \frac{p^4}{4})^{1/2} - \frac{p^2}{2}]^{1/2} \\ s = [(q^4 + \frac{p^4}{4})^{1/2} + \frac{p^2}{2}]^{1/2} \end{cases} \quad (6)$$

In equation (6),

$$p^2 = T/EI \quad (7)$$

$$q^4 = m\omega^2/EI \quad (8)$$

where ω is the circular frequency of conductor vibration (rad), and the equation (9) can be obtained by transforming equation (5).

$$\varepsilon_{\max} = \frac{\sqrt{2}Dy_{\max}}{4} \sqrt{H} \sqrt{H - \frac{p^2}{2}} \quad (9)$$

In equation (9), ε_{\max} is the maximum dynamic bending strain of the conductor at the outlet of the clamp; D is the conductor diameter (m); H is an intermediate variable, which can be described as follows,

$$H = \sqrt{q^4 + p^4/4} \quad (10)$$

1.2 Calculation of dynamic bending stiffness

For the erected conductor in test, its diameter, tension and mass per unit length are known, and the antinode amplitude, vibration frequency and the maximum strain at the outlet of clamp can be obtained through experimental measurement. By substituting these parameters into equation (9), the dynamic bending stiffness of the conductor can be calculated. In this paper, we use the dichotomy method to calculate the dynamic bending stiffness, which meets a given accuracy ζ . The solution flow is shown in Fig. 2.

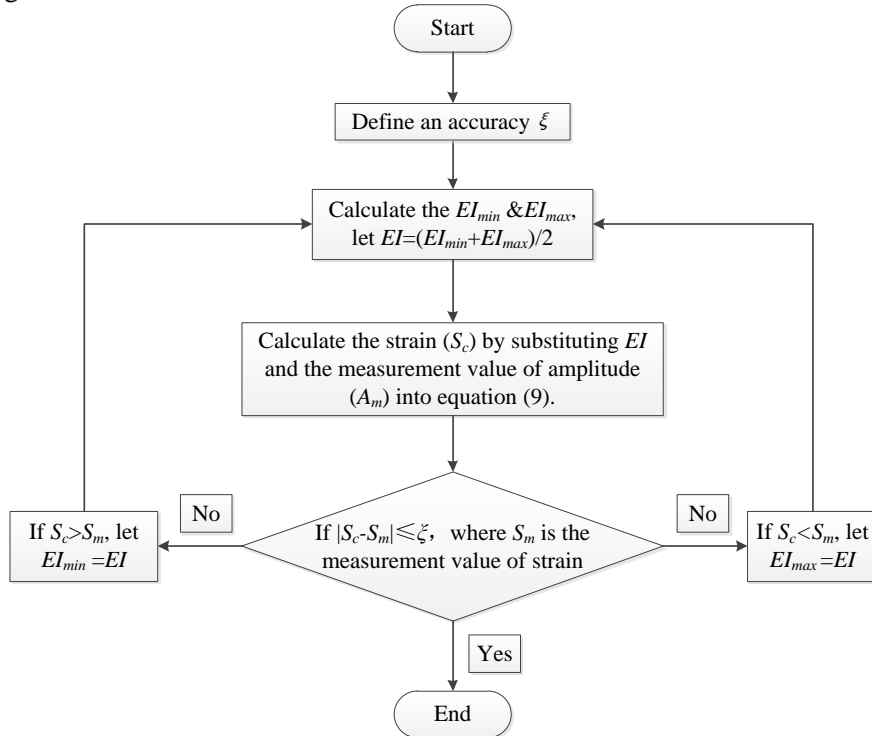


Fig. 2 Flow chart of bending stiffness solution

There are some specific steps in Fig. 2,

- 1) Define an accuracy ζ , in this paper $\zeta = 0.001$.
- 2) EI_{min} and EI_{max} are used to represent the minimum and the maximum dynamic bending stiffness respectively. At the beginning, it is assumed that the value of EI_{min} is 0 and the value of EI_{max} is estimated by the method that will be shown in subsection 2.1.
- 3) Take the midpoint of EI_{min} and EI_{max} , which means $EI = (EI_{min} + EI_{max}) / 2$. Substitute EI and the amplitude (A_m) measured in the test into equation (9) to calculate the maximum bending strain (S_c) at the outlet of conductor clamp.
- 4) Compare S_c with the measured value (S_m), when $|S_c - S_m| > \zeta$, it needs to repeat step 3). It should be noted that if $S_c > S_m$, the value of EI will instead of the value of EI_{min} for the next iteration, and if $S_c < S_m$, the value of EI is assigned to EI_{max} . Until $|S_c - S_m| \leq \zeta$, the EI that meets the accuracy can be obtained.

2. MEASUREMENT AND RESULTS ANALYSIS

2.1 Conductor parameters

The conductor used in this paper is composed of aluminium single wires with trapezoidal section and composite core. Its section is shown in Fig. 3. The density of composite material is 2000 kg/m^3 , which is lower than that of aluminium. Therefore, the mass per unit length of this kind of conductor is less than the aluminium conductor steel reinforced with a same section area. The parameters of the conductor are shown in Table I.

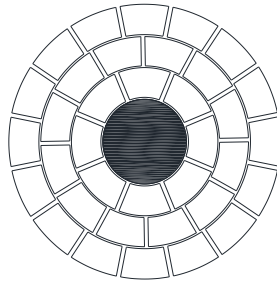


Fig. 3 Conductor section

Table I Conductor parameters

| | |
|-------------------------------|-----------------------|
| Conductor type | JLRX/F1B-500/55 |
| Diameter of conductor | 27.6 mm |
| Section area | 556.7 mm ² |
| Mass per unit length | 1.492 kg/m |
| Diameter of composite core | 8.50 mm |
| Number of aluminum wires | 36 |
| Rated tensile strength (RTS) | 148 kN |
| Comprehensive elastic modulus | 60.61 Gpa |

The comprehensive elastic modulus is calculated by the elastic modulus of aluminium and fiber composite core, which can be described as follows [3],

$$E_c = \frac{E_f S_f + E_a S_a}{S_f + S_a} \quad (11)$$

where E_c is the comprehensive elastic modulus of the conductor (Pa); E_f is the elastic modulus of carbon fiber core (Pa); S_f is the section area of the carbon fiber core (m²); S_a is the section area of the aluminium (m²).

It is worth noting that a method for estimating the maximum dynamic bending stiffness by using the product of the comprehensive elastic modulus and the area moment of inertia is proposed to simplify the calculation. The calculation method is as follows,

$$EI_e = E_c I_c \quad (12)$$

$$I_c = \frac{\pi d_{eq}^4}{64} \quad (13)$$

$$d_{eq} = \sqrt[4]{4(S_f + S_a)/\pi} \quad (14)$$

where EI_e is the estimated value of dynamic bending stiffness (N.m²), I_c is the area moment of inertia of conductor (m⁴), and d_{eq} is the equivalent diameter of conductor (m).

2.2 Test measurement

The span length of aeolian vibration simulation test bench is 140 m. The conductor is erected on the test bench with a certain tension, and rigid square-faced bushing is used at both ends to fix the conductor. As shown in Fig. 4, the vibration shaker is arranged at the right end of the test bench, which can output sinusoidal signal to excite the conductor and simulate the aeolian vibration of the conductor. The displacement sensor is arranged near the left end. The vibration waveform of the conductor will change with the changing of vibration frequency. It is necessary to move the sensor to ensure that it can measure the antinode amplitude of the first half wave of the conductor. The strain sensors are pasted on the outermost strand at the outlet of the square-faced bushing, as shown in Fig. 5.

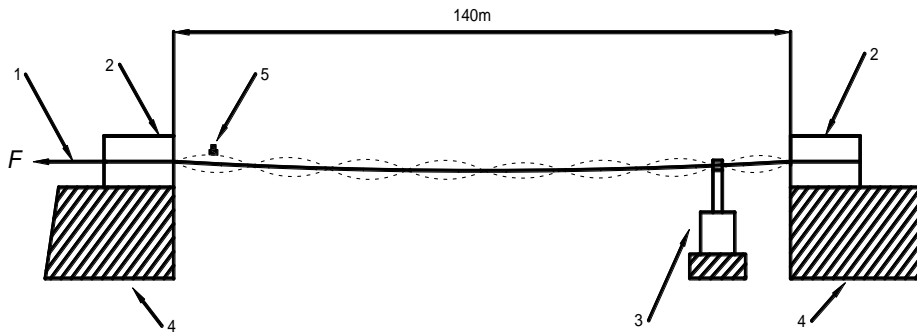


Fig. 4 Schematic diagram of test bench. Where 1 is constant tension device, 2 is rigid square-faced bushing, 3 is vibration shaker, 4 is the foundation, 5 is displacement sensor.

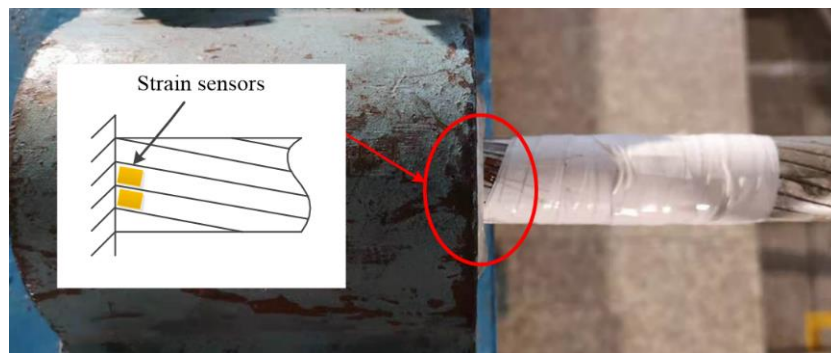


Fig. 5 Strain sensors on the conductor at the end

The conductor is excited with different frequencies and amplitudes. When the conductor vibrates stably and the value of strains (0-peak) at the outlet of square-faced bushing is close to 70 $\mu\epsilon$, 140 $\mu\epsilon$, 210 $\mu\epsilon$, 280 $\mu\epsilon$ and 350 $\mu\epsilon$, the actual strain value and its corresponding amplitudes of the conductor

are recorded. The dynamic bending stiffness of the conductor can be obtained by combining the measured values with the method described in subsection 1.

2.3 Test results and analysis

Under the conditions of 18.4% RTS, 22.4% RTS and 26.7% RTS, the conductor is excited by sinusoidal signal, of which the frequencies are 20 Hz, 30 Hz, 40 Hz, 50 Hz and 60 Hz respectively. The recorded amplitude and strain values are shown in Table II.

Table II The test results of strain and amplitude

| Frequency (Hz) | 18.4% RTS | | 22.4% RTS | | 26.7% RTS | |
|----------------|--------------------------|----------------|--------------------------|----------------|--------------------------|----------------|
| | Strain ($\mu\epsilon$) | Amplitude (mm) | Strain ($\mu\epsilon$) | Amplitude (mm) | Strain ($\mu\epsilon$) | Amplitude (mm) |
| 20 | 71.91 | 2.09 | 69.26 | 1.75 | 74.58 | 2.05 |
| | 141.35 | 4.27 | 139.98 | 3.60 | 137.03 | 3.91 |
| | 213.49 | 6.67 | 264.43 | 6.82 | 220.24 | 6.34 |
| | 279.29 | 8.67 | 300.96 | 7.77 | 279.18 | 8.44 |
| | 315.14 | 9.50 | 348.85 | 9.07 | 329.94 | 10.43 |
| 30 | 73.82 | 1.28 | 76.03 | 1.26 | 69.44 | 1.28 |
| | 138.66 | 2.42 | 147.24 | 2.44 | 145.68 | 2.71 |
| | 220.85 | 3.93 | 214.34 | 3.48 | 227.32 | 4.17 |
| | 288.38 | 5.19 | 283.03 | 4.55 | 282.18 | 5.15 |
| | 354.41 | 6.56 | 354.21 | 5.67 | 358.18 | 6.52 |
| 40 | 68.83 | 0.86 | 68.35 | 0.80 | 75.56 | 0.99 |
| | 142.44 | 1.68 | 131.87 | 1.51 | 144.65 | 1.86 |
| | 205.67 | 2.47 | 212.14 | 2.40 | 223.02 | 2.94 |
| | 283.25 | 3.45 | 308.92 | 3.47 | 286.05 | 3.77 |
| | 412.29 | 5.30 | 375.16 | 4.21 | 348.22 | 4.61 |
| 50 | 71.72 | 0.68 | 84.92 | 0.74 | 77.79 | 0.78 |
| | 142.22 | 1.40 | 146.93 | 1.22 | 139.63 | 1.41 |
| | 209.37 | 2.01 | 217.97 | 1.86 | 243.51 | 2.46 |
| | 278.18 | 2.74 | 288.72 | 2.48 | 320.96 | 3.18 |
| | 352.22 | 3.38 | 358.41 | 3.07 | 373.75 | 3.69 |
| 60 | 80.96 | 0.55 | 72.52 | 0.49 | 72.45 | 0.50 |
| | 138.84 | 0.88 | 170.20 | 1.13 | 145.58 | 1.00 |
| | 212.51 | 1.32 | 214.17 | 1.44 | 216.28 | 1.46 |
| | 274.03 | 1.81 | 282.80 | 1.88 | 276.93 | 1.87 |
| | 296.22 | 1.95 | 346.36 | 2.24 | 331.07 | 2.31 |

By substituting the measured data into equation (9), the conductor stiffness under different test conditions can be calculated. For the convenience of analysis, we define the ratio of the calculated value of dynamic bending stiffness to the maximum value estimated by equation (12) as the stiffness coefficient. The stiffness coefficient calculated by the test data is shown in Fig. 6. It is shown that the law of the variation of the conductor stiffness coefficient with the amplitude is not obvious. According to Fig. 6 (a) ~ (c), the distribution of the stiffness coefficient in the coordinate system tends to be concentrated first and then dispersed with the increase of tension. However, the change of stiffness coefficient with vibration frequency has a clear regularity. The stiffness coefficient of conductor under the same frequency is relatively concentrated.

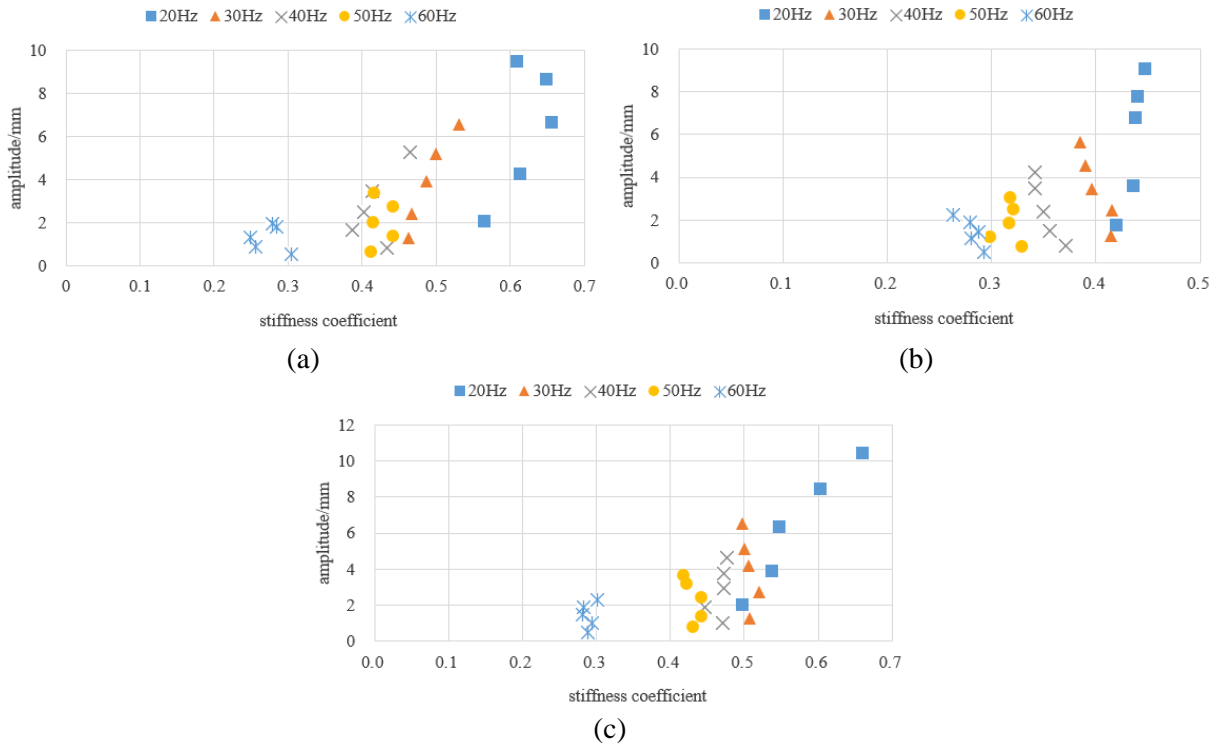


Fig. 6 The stiffness coefficient under different conditions. Where (a), (b) and (c) are the stiffness coefficients under the condition of 18.4% RTS, 22.4% RTS and 26.7% RTS respectively.

3. EVALUATION METHOD OF DYNAMIC BENDING STIFFNESS

The average value of conductor stiffness coefficient under the same frequency is calculated. As shown in Fig. 7, the conductor stiffness coefficient has a linear relationship with vibration frequency, and the conductor stiffness coefficient gradually decreases with the increase of vibration frequency. By fitting the stiffness coefficient of conductor at different frequencies, a linear function relationship between stiffness coefficient and frequency is obtained. Using this linear function, the approximate stiffness coefficient of conductor at different frequencies can be calculated to obtain the dynamic bending stiffness of conductor.

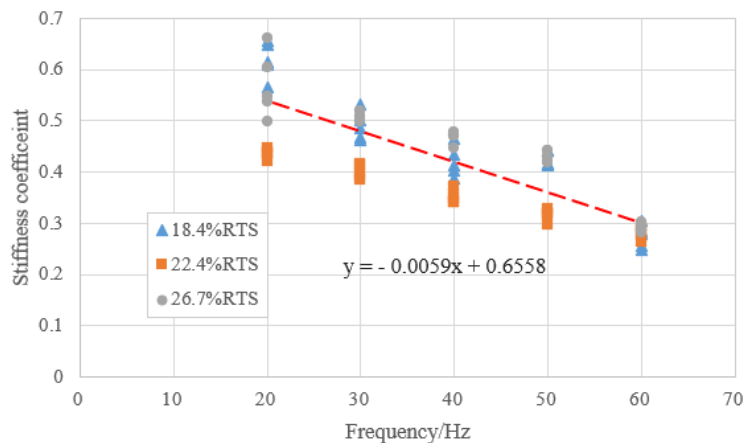


Fig. 7 The average values of stiffness coefficient and its fitting

By using the functional relationship described in Fig. 7, the dynamic bending stiffness of the conductor at each frequency is obtained and shown in Table III. The results show that the dynamic

bending stiffness of the conductor with formed wires is mostly less than $0.5EI_{max}$, a value advocated by CIGRE [4].

Table III The calculate result of dynamic bending stiffness

| Frequency(Hz) | Stiffness coefficient | Dynamic bending stiffness (N.m ²) |
|---------------|-----------------------|---|
| 20 | 0.54 | 928.46 |
| 30 | 0.48 | 826.60 |
| 40 | 0.42 | 724.74 |
| 50 | 0.36 | 622.89 |
| 60 | 0.30 | 521.03 |

The stiffness value is substituted into the dynamic bending strain model described in subsection 1.1, and the result is compared with the measured one to verify the accuracy of the function in Fig. 7. The calculation result is shown in Fig. 8, where the maximum relative error is less than 12%. Therefore, the use of this method to determine the dynamic bending stiffness of the conductor with formed wires can ensure a certain accuracy when performing fatigue test (see reference [5]) or calculating the aeolian vibration of the conductor.

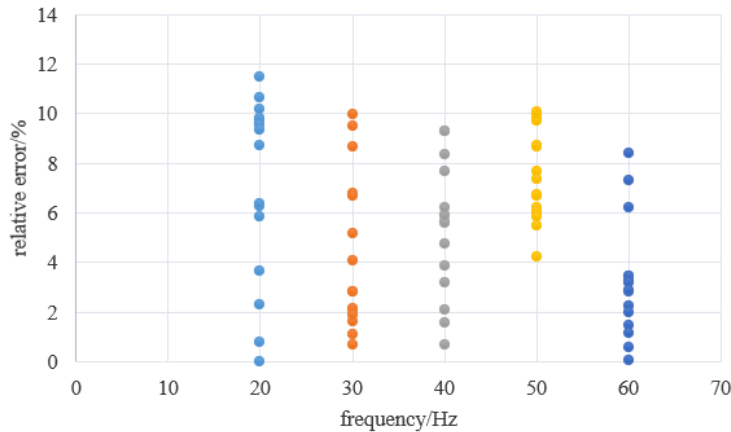


Fig. 8 Relative error of the calculation result

4. CONCLUSION

In order to study the dynamic bending stiffness of the typical overhead conductor with formed wires, the expression of dynamic bending strain at the conductor clamp outlet is derived from the aeolian vibration model of conductor that simply supported at both ends, which is used to approximately characterize the strain mathematical model in experimental measurement. Based on the theoretical model and experimental data, the variation law of dynamic bending stiffness of the typical conductor with its tension and vibration frequency is obtained.

The function relationship of the stiffness coefficient of the typical overhead conductor with frequency is obtained by fitting. Based on the function relationship, the strain at the outlet of conductor clamp is calculated again for different tensions, amplitudes and vibration frequencies, and the accuracy and error of the dynamic bending stiffness evaluated by the proposed method are obtained.

The method in this study can be used as a reference for determining the dynamic bending stiffness value of other conductors, including other types of conductors with formed wires and the conventional overhead conductors. It is of great significance for the aeolian vibration numerical simulation and the fatigue test of conductors.

BIBLIOGRAPHY

- [1] Claren R., Diana G.. *Mathematical Analysis of Transmission Line Vibration* [J]. IEEE Transactions on Power Apparatus and Systems, 1969, 88(12):1741-1771.
- [2] Hong W., Yibing L., Yuming D., etc. *The Study of Conductor Fatigue Test Amplitude of Overhead Lines* [J]. Proceedings of the CSEE, 2008, 28(4): 123-128.
- [3] Jiancheng W.. *Application Technology of Overhead Conductor* [M]. Beijing, China electric power press, 2015: 62-65.
- [4] CIGRE. *Aeolian Vibration on Overhead Lines* [C]. International Conference on large high tension electric systems, Paris, France, 1970.
- [5] IEC 62568 *Overhead Lines-Method for Fatigue Testing of Conductors* [S]. Switzerland, IEC, 2015.